

Quarterly Progress Report

N01-NS-1-2333

Restoration of Hand and Arm Function by Functional Neuromuscular Stimulation

Period covered: October 1, 2001 to December 31, 2001

Principal Investigator: Robert F. Kirsch, Ph.D.

Co-Investigators:

Patrick E. Crago, Ph.D.
P. Hunter Peckham, Ph.D.
Warren M. Grill, Ph.D.
J. Thomas Mortimer, Ph.D.
Kevin L. Kilgore, Ph.D.
Michael W. Keith, M.D.
David L. Wilson, Ph.D.

Joseph M. Mansour, Ph.D.
Jeffrey L. Duerk, Ph.D.
Wyatt S. Newman, Ph.D.
Harry Hoyen, M.D.
John Chae, M.D.
Jonathon S. Lewin, M.D.
Richard Lauer, Ph.D.

Case Western Reserve University
Wickenden 407
10900 Euclid Avenue
Cleveland, OH 44106-7207
216-368-3158 (voice)
216-368-4969 (FAX)
rfk3@po.cwru.edu

Contract abstract

The overall goal of this contract is to provide virtually all individuals with a cervical level spinal cord injury, regardless of injury level and extent, with the opportunity to gain additional useful function through the use of FNS and complementary surgical techniques. Specifically, we will expand our applications to include individuals with high tetraplegia (C1-C4), low tetraplegia (C7), and incomplete injuries. We will also extend and enhance the performance provided to the existing C5-C6 group by using improved electrode technology for some muscles and by combining several upper extremity functions into a single neuroprosthesis. The new technologies that we will develop and implement in this proposal are: the use of nerve cuffs for complete activation in high tetraplegia, the use of current steering in nerve cuffs, imaging-based assessment of maximum muscle forces, denervation, and volume activated by electrodes, multiple DOF control, the use of dual implants, new neurotization surgeries for the reversal of denervation, new muscle transfer surgeries for high tetraplegia, and an improved forward dynamic model of the shoulder and elbow. During this contract period, all proposed neuroprostheses will come to fruition as clinically deployed and fully evaluated demonstrations.

Summary of activities during this reporting period

The following activities are described in this report:

- *Measurement of human upper extremity nerve diameters and branch-free lengths.*
- *Magnetic resonance imaging of muscles of the human elbow and shoulder.*
- *A robotic facility for evaluation of control sources to restore arm function via FNS to individuals with high level tetraplegia.*
- *Wireless data acquisition module for use with a neuroprosthesis.*
- *Rapid prototyping and real-time control for functional electrical stimulation (FES).*

Measurement of human upper extremity nerve diameters and branch-free lengths.

Contract sections:

E.1.a.i Achieving Complete and Selective Activation Via Nerve Cuff Electrodes

E.2.a.i Selective Activation of Elbow and Shoulder Muscles by Nerve Cuff Electrodes

Abstract

The ability to selectively activate peripheral nerve trunk fascicles using nerve cuff electrodes is well established. In the effort to combine several upper extremity functions into a single neuroprosthesis it is desirable to use this technology for activation of specific muscles. Anatomical and fascicular topography studies of the upper extremity nerves are being conducted so that implant sites that maximize success can be identified. The anatomical studies include measurements of the diameters and branch free lengths of the nerves on four complete brachial plexus groups. The use of lipophilic dyes in the fascicular topography studies is being explored with the focus on increasing the maximal tracing distances of these dyes in fixed tissue so that their utility in this study can be maximized.

Introduction

The ability to use multiple contact spiral nerve cuff electrodes to achieve selective activation of peripheral nerve trunk fascicles has been demonstrated. The key developments in this technology were a cuff that expands and contracts to provide a snug, non-compressive fit on the nerve [Naples et al., 1988], and a distributed array of contacts that allows the performance of the electrode to be independent of the position of the cuff around the nerve [Veraart et al., 1993. Grill and Mortimer 1996a]. These studies showed that a multiple contact cuff is able to activate selectively and maximally individual fascicles of a nerve trunk without prior reference to the fascicular structure of the nerves. The results of these studies were replicated in long-term chronically implanted electrodes which demonstrated that this selectivity is maintained over time [Grill and Mortimer, 1998]. Overall, the results indicate that a multi-contact nerve cuff electrode implanted on an upper extremity motor nerve trunk will enable selective and graded activation of multiple muscles.

The ability to activate selectively fascicles of a peripheral nerve has several potential applications in an upper extremity neuroprosthesis. Nerve cuff electrodes are also useful when the shape of the muscle is complex or the innervation pattern of the muscle is branched. Figure 1 shows the possible nerves that have been targeted for cuff electrodes and the muscles that we desire to be able to stimulate with these cuff electrodes.

To maximize the success of the nerve cuff electrodes and achieve selective activation of the desired muscles, it is necessary to study the anatomy and fascicular structure of the upper extremity motor nerves to identify implant sites and lead routing paths. Cadaver dissections of upper extremity nerves are being used in this study. The anatomical study includes measurements of the diameters and branch-free lengths of the nerves to see if there is the necessary room for multi-contact cuff electrodes.

The fascicle study is important so that accurate computer models can be created to simulate the cuff stimulation and predict whether the desired selective muscle stimulations can be achieved. A pilot study of fascicle mapping that consisted of cross-sectioning an excised radial nerve showed that it is extremely difficult to accurately follow the changing fascicular topography. In addition to this problem, once fascicles merge it becomes impossible to identify one muscle branch from another or make predictions on whether distinct branch groupings can be found inside of a large fascicle that may branch into several muscle groups. The use of lipophilic carbocyanine dyes to trace distinct muscle branches is being investigated to overcome the limitations of standard cross-sectioning.

Nerve	Muscles To Be Stimulated
Long Thoracic	Serratus Anterior
Suprascapular	Supraspinatus
	Infraspinatus
Thoracodorsal	Latissimus dorsi
Radial	Triceps excluding long head
	ECRL
	ECRB
	ECU
Axillary	Deltoid
	Teres Minor
L. Subscapular	Subscapularis
	Teres Major
U. Subscapular	Subscapularis
Musculocutaneous	Biceps
	Brachialis

Figure 1.
Nerves targeted for cuff electrodes

Dissection Methods

The cadaver dissections were performed using blunt dissection techniques. The brachial plexus, its branches, and the branches of the axillary, musculocutaneous, and radial nerve were identified and tagged. Any irregularities were noted and photographed. Length measurements were done using calipers while the diameters of the nerves were calculated after using a suture to measure the circumference and assuming a circular cross section. Once these measurements were completed the nerves were excised en masse with muscle branches being tagged with sutures for identification purposes. The nerves were then stored at 4 °C for future studies of their fascicular structure.

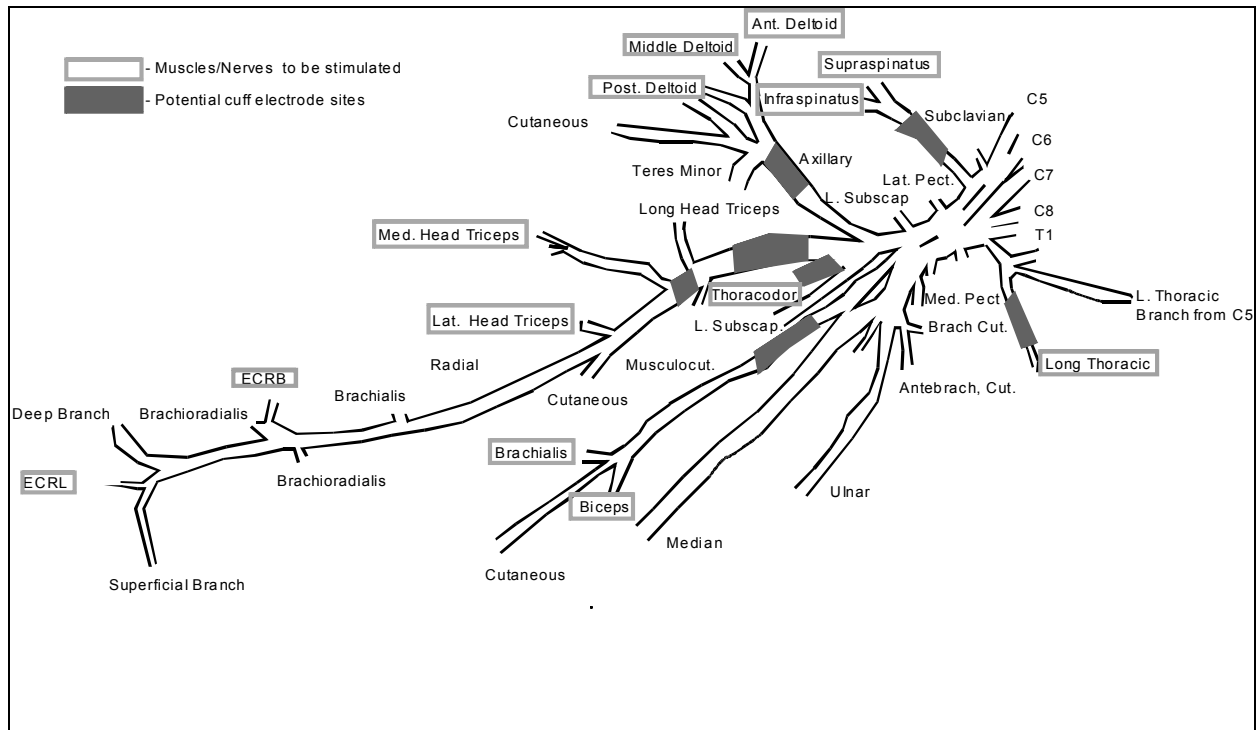


Figure 2. Right upper extremity nerves (9802R)

Dissection Results

Four brachial plexuses have been dissected with branch-free lengths and circumference measurements taken. Figure 2 shows one of the complete plexus dissections with the stimulation goals and the most likely cuff electrode sites highlighted. Measurements of the branch free lengths and nerve diameters for these potential cuff electrode sites have been taken to see if they meet the minimum requirements for multi-contact electrodes. For current multi-contact electrodes to be used a minimum branch free length of 2 cm and a minimum diameter of 1.6 mm are necessary.

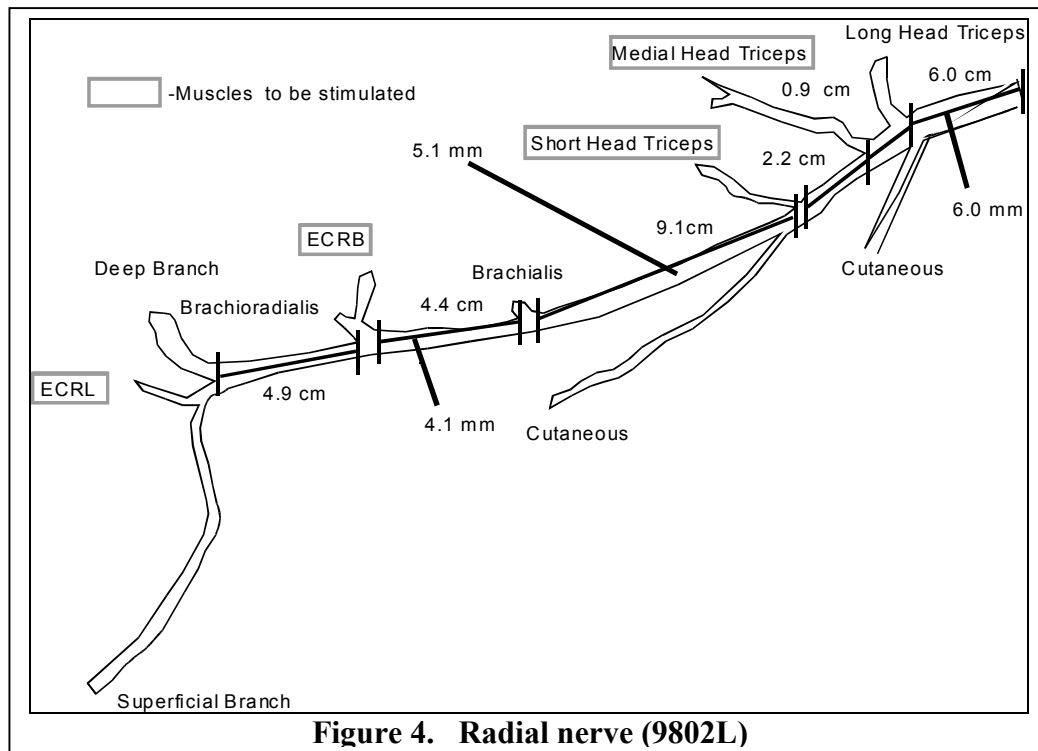
Figure 3 shows measurements that have been obtained for potential cuff sites. The suprascapular, axillary, and musculocutaneous nerves all met the minimum requirements for branch free lengths and diameters at the most desirable cuff electrode sites. The musculocutaneous nerve results show that it appears that the cuff electrode can be placed below the coracobrachialis branch to avoid unwanted stimulation of the coracobrachialis.

Measurements were also taken for the long thoracic, thoracodorsal, and upper and lower subscapular nerves. These nerves provide ample branch free lengths but do not always meet the minimum diameter requirements for a multi-contact cuff electrode. These nerves innervate a single muscle making selective stimulation unnecessary, so single contact cuff electrodes that can be made for smaller diameter nerves can be used.

Nerve	Branch Free Length (cm)			Diameter (mm)		
	Min	Mean	Max	Min	Mean	Max
Suprascapular	5.3	5.6	6.1	1.6	1.8	2
Axillary	5.5	5.8	6.4	2.5	2.8	3.2
Musculocutaneous (post-coracobrachialis branches)	4.9	5.2	5.5	2	2.4	2.6
Radial (pre-long head tricep branches)	5.9	6.3	6.7	3.5	3.8	4
Radial (post-long head tricep branches)	0.9	1.6	2.2	3.3	3.5	3.9

Figure 3. Branch free lengths and diameters

Of the nerves targeted for cuff electrodes and selective stimulation, the radial nerve poses the greatest challenges. The radial nerve (Figure 4) innervates a large number of muscles as well as provides sensory information for parts of the forearm and hand. In addition, the selective stimulation goals for the radial nerve involve a greater number of muscles (medial and short heads of triceps, ECRB, ECU) compared to the other identified target areas. It would be desirable to place the radial cuff electrode below the long head of triceps branch because stimulation of this portion of the triceps will result in unwanted shoulder actions. Placing the cuff below the long head of triceps branch would preclude stimulation of that muscle and simplify the challenge of selective stimulation in the radial nerve. The current results (Figure 3), however, show that the necessary branch-free length is not always available between the long



head triceps branch and the medial triceps branch. This means the cuff electrode for the radial nerve will likely have to be located above the long head triceps branch adding complexity to the selective stimulation.

Two of the dissected brachial plexus groups will be sectioned using conventional methods. This cross-sectioning will focus on two key areas: likely cuff electrode sites and areas immediately preceding the branching to muscles that we desire to stimulate. Information about the internal topography of the radial nerve is of the highest priority in this study since the radial nerve poses the greatest challenges for achieving selective stimulation. As previously mentioned, the pilot study of cross-sectioning showed that it was difficult to follow fascicle groups from one section to another. To solve this problem, higher frequency sectioning will be used (compared to the pilot study in which 1cm intervals were used).

Lipophilic Nerve Tracing

Retrograde tracing using lipophilic dyes has been used in postmortem aldehyde-fixed nerve fibers (Honig and Hume 1986, 1989; Godement et al. 1987; Honig 1993). The main limitations of these dyes has been the limited maximal tracing distance that can be achieved due to the slow diffusion rate that can be achieved in fixed tissue. This slow diffusion rate is due to the cross-linking of proteins that occurs during the aldehyde fixation process (Sparks et al. 2000). Lukas et al. found maximal tracing distance for DiI (1,1'-dioctadecyl-3,3,3'-tetramethylindocarbocyanine perchlorate), DiO(3,3'-dioctadecyloxa-carbocyanine perchlorate), and DiA (4-(4-dihexadecylamino)styryl)-*n*-methylpyridinium iodide) for fixed human tissue. Their results found that incubation at 37°C for 12-15 weeks provided optimal tracing distances of 28.9 ±2.2 mm for DiI with DiO and DiA having optimal tracing distances varying from 15 to 20 mm.

Lukas's optimal distances are consistent with other reports and fall well below the distances that would be necessary for our needs. In the radial nerve, tracing distances of at least 200 mm would be desirable for us to be able to identify the muscle branches that are targeted for selective activation at the most likely cuff electrode sites. Two different approaches are being considered to increase the tracing distances of the lipophilic dyes.

The first approach hinges upon the fact that a number of these dyes including DiI, DiO and DiA are cationic. It may be possible to place the nerves that are being traced in DC electric fields to increase the force behind the diffusion process. Our hypothesis is that this will speed up the diffusion of the dyes in the nerve tissue and increase the maximal tracing distances that can be achieved. An experiment to test this concept is currently underway.

The second approach is to use unfixed fresh tissue. Sparks et al. (2000) reported diffusion rates of 1 mm/hour for DiI when fresh nerve tissue was used. They were able to reach maximal tracing distances of 40 mm in 40 hours before the tissue was then fixed for cross-sectioning. This diffusion rate is several magnitudes of order greater than any previously reported in fix tissue. It may be possible to diffuse for time spans longer than 40 hours prior to fixation to increase the maximal tracing distances.

Next Quarter

During the next quarter we will complete dissection of 2 additional brachial plexuses and pursue experiments to enhance the diffusion of lipophilic dyes using exogenous electric fields. The results of the attempts to use electric fields to increase the tracing distance of the lipophilic dyes will dictate the direction of the rest of the anatomical study.

References

- Godement P, Vanselow J, Thanos S, Bonhoeffer F. A study in developing visual systems with a new method of staining neurons and their processes in fixed tissue. *Development* 1987;101:697-713.
- Grill WM, Mortimer JT. Non-invasive measurement of the input-output properties of peripheral nerve stimulating electrodes. *J Neurosci Meth* 1996;65:43-50.
- Grill WM, Mortimer JT. Stability of the input-output properties of chronically implanted multiple contact nerve cuff stimulating electrodes. *IEEE Trans Rehab Eng* 1998;6:364-73.
- Honig MG, Hume RI. Di-I and Di-O: versatile fluorescent dyes for neuronal labeling and pathway tracing. *Trends Neurosci* 1989;12:333-35.
- Honig MG, Hume RI. Fluorescent carbocyanine dyes allow living neurons of identified origin to be studied in long-term cultures. *J Cell Biol* 1986;103:171-87.
- Honig MG. DiI labeling. *Neurosci Protocols* 1993;50:1-20.
- Lukas J, Aigner M, Denk M, Heinzl H, Burian M, Mayr R. Carbocyanine Postmortem Neuronal Tracing: Influence of Different Parameters on Tracing Distance and Combination with Immunocytochemistry. *J Histochem & Chem* 1998;46(8):901-10.
- Naples GG, Mortimer JT, Sheiner A, Sweeney JD. A spiral cuff electrode for peripheral nerve stimulation. *IEEE Trans Biomed Eng* 1988;35:905-16.
- Sparks DL, Lue L, Martin TA, Rogers J. Neural tract tracing using Di-I: a review and a new method to make fast Di-I faster in human brain. *J Neurosci Meth* 2000;103:3-10.
- Veraart C, Grill WM, Mortimer JT. Selective control of muscle activation with a multipolar nerve cuff electrode. *IEEE Trans Biomed Eng* 1993;40:640-53.

Magnetic resonance imaging of muscles of the human elbow and shoulder

Contract section: E.1.a.ii.4.1 Model customization: muscle volume estimates via MRI

Abstract

In this project, we are using magnetic resonance imaging (MRI) to non-invasively determine the muscle volume of the shoulder in individuals with high tetraplegia. Muscle volume has been found [Fukunga et al. 1992; Kawakami et al. 1994] to be a good predictor of Physiological Cross Section Area (PCSA) and, hence, maximum muscle force. Individuals with high tetraplegia have extensive paralysis of muscles of the upper extremity, and may have widespread denervation of elbow and shoulder muscles. Characterization of the residual force generating capacity of these muscles, either by voluntary contractions or by FNS of paralyzed muscle fibers, is essential for determining the ultimate feasibility of using FNS in these individuals. It is not reasonable to individually stimulate each of the more than 30 muscles of the shoulder and elbow just to determine the feasibility of a neuroprosthesis, so we will approximate the maximum muscles forces via MRI-based volume measurements.

Methods

The method of analysis used in this project consists of three basis steps: image post processing, muscle boundary outlining, and volume estimation. These steps were applied to two different data sets: histological sections obtained from the Visible Human project, consisting of

digital photographs of actual cross-sections of the shoulder region, and the other obtained from an MRI scan of the same area in an able-bodied subject. Both data sets contained transverse cross sections of the human shoulder. All data analysis was performed using Analyze Biomedical Engineering Software developed by the Mayo Clinic, run with Windows 2000.

The Visible Human data obtained from the Complete Visible Human CD was used as it represents a close to ideal data set for this region, and could be used as a template for practicing the techniques developed here. In addition, the Atlas of the Visible Human Male (Spitzer and Whitlock 1997) contained a complete list of muscle identifications for the Visible Human data set. This allowed muscles of interest to be identified quickly and accurately both in this data set and in the MRI scans, by comparing the structures.

The Visible Human images were reduced in size and converted from color images to gray scale to better correspond with the appearance of the MRI data set. The muscle chosen for this initial testing was the subscapularis, being relatively large and easily identifiable in the data set. At first, attempts were made at applying an automatic border detection algorithm to find the outlines of the muscles. With the low contrast of some of the slices, however, it soon became necessary to trace the boundaries manually. The semi-manual method developed for greatest efficiency in tracing was to begin in the middle of the data set, where the subscapularis was most prominent. The Analyze software allowed for manually tracing around the boundary of the muscle using its "Region of Interest" tool. This boundary could then be copied to subsequent slices in both directions and modified to fit the new muscle cross section, which usually varied only slightly from slice to slice. This process was repeated for all of the slices containing any visible trace of the subscapularis boundary. In order to accommodate sections where the muscle boundary was not clearly visible, the traced border from the previous slice was left unmodified. The final result was a stack of tracings defining the contours of the muscle. This same procedure was then performed on the subscapularis of the MRI data set, identified by cross-referencing with the Visible Human images.

Before this contour tracing was completed, it was necessary to check the boundaries for accuracy. The transverse sections were therefore recalculated to produce slices in both the sagittal and coronal directions. The muscle contours could be double-checked in this mode by visualizing the boundaries of the muscle from different viewpoints. Any visible inaccuracies in the muscle borders were then corrected until the contours in all views were acceptable.

Through use of the Volume Rendering function of the Analyze software, two tasks could be accomplished. The first was a diagnostic, in which the full three-dimensional shape of the muscle could be visualized from different angles. By comparing this with known muscle shapes, it could be determined whether the muscle boundary was defined accurately or not. Secondly,

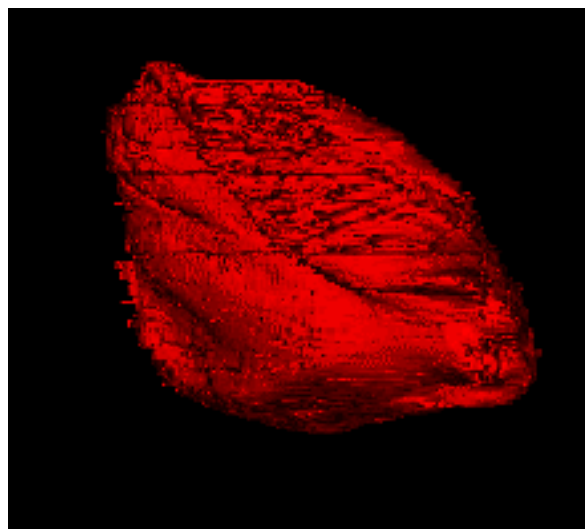


Figure 5. An example three-dimensional volumetric rendering of the subscapularis muscles from the Visible Human data set.

the volume of the three-dimensional shape, in units of 3-D pixels or “voxels” could be calculated.

These processes were repeated for several other muscles in the shoulder from the MRI data set: the serratus anterior, the infraspinatus, and the supraspinatus.

Results

Within a reasonable learning time, it became possible to trace a complete muscle boundary in less than half an hour, an important aspect in making this useful for clinical analysis. The process worked very well for the ideal sample of the Visible Human data, producing smooth boundaries and an accurate shape. An example of the three-dimensional rendering of the subscapularis can be seen in Figure 5.

The task of identifying muscle contours was much more difficult to determine in the MRI data set, primarily due to large contrast changes over the width of the image. Histogram resampling fixed this difficulty to some extent, but the boundaries of many of the muscles that extended laterally away from the torso into the upper were blurred enough to make border identification impossible. Nonetheless, a reasonable boundary could be determined for some muscles, an example of which (subscapularis) can be seen in Figure 6.



Figure 6. An example of a subscapularis boundary tracing in the Analyze program, taken from the MRI data set.

At this point, the only completely successful volume estimate has been of the subscapularis muscle. In both the Visual Human set and the MRI data set, this muscle was well bounded by bone and clearly visible connective tissue. Other muscle estimates were not possible, for several reasons. The edges of the serratus anterior are very difficult to determine because this muscle is very narrow and its border is often indistinguishable from the nearby ribcage bones and subscapularis border. The serratus anterior could not be traced completely in either the Visual Human set or the MRI data set. The infraspinatus and supraspinatus muscles are much more obvious in outline, and it was possible to find them in the Visual Human set with some amount of accuracy. However, the MRI set was limited by a severe darkening and loss of contrast over the most lateral regions of these muscles. As a result, the borders were completely unidentifiable in our current images.

As mentioned above, automatic border detection appears to be impractical at this point. The low contrast in some of the MRI slices resulted in a need for manual estimation of the border in some regions. It is possible that the borders could be made clear enough to attempt this approach again with further optimization of the image quality.

Next quarter

The next step in the development of this muscle volume estimation technique is to acquire an improved MRI data set. It was obvious shortly after obtaining the current set that the image deteriorated in the lateral areas of the torso and upper arm. Methods for improving the image quality have been identified and will be employed in the next experiment. Improved images should significantly expand the number of muscles whose volumes can be estimated.

References

- Fukunaga, T., Roy, R.R., Shellock, F.G., Hadgson, J.A., Day, M.K., Lee, P.L., Kwong-Fu, H., Edgerton, V.R. Physiological cross-sectional area of human leg muscles based on magnetic resonance imaging. *J. Orthop. Res.* 10: 928-934, 1992.
- Kawakami, Y., Nakazawa, K., Fujimoto, T., Nozaki, D., Miyashita, M., Fukunaga, T. Specific tension of elbow flexor and extensor muscles based on magnetic resonance imaging. *Eur. J. Appl. Physiol.* 68: 139-147, 1994.
- Spitzer, V.M. and Whitlock, D.G. *National Library of Medicine Atlas of the Visible Human Male*. Jones & Bartlett Pub, 1997.

A Robotic Facility for Evaluation of Control Sources to Restore Arm Function via FNS to Individuals with High Level Tetraplegia

Contract section: E.1.a.iv Command sources for high tetraplegia

Abstract

The purpose of this project is to develop a robot system to emulate the kinematics and dynamics of a human arm, so that it enables faster evaluations of a larger number of candidate controllers of an advanced neuroprosthetic system.

Methods and Results

During this quarter, a robot mounting stand with safety shield has been designed and fabricated. Impact resistance of the safety shield has also been verified by tests. EOG and EMG signals have been compared as human-computer interface means for the robot system. A robot controller using EOG/EMG as input has been designed and tested. Some initial studies of control schemes are being implemented and benchmarked.

Robot Mounting Stand and Safety Shield

A robot test stand was designed and fabricated for mounting the robot horizontally with its base at shoulder height, enabling an approximation to human arm mobility, as shown in Figure 7. Tests show that the test stand, as designed, is capable of supporting the static and dynamic loads of the 300-lb robot.

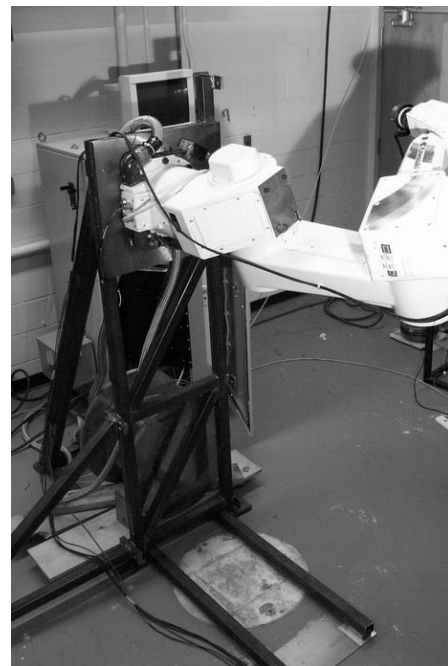


Figure 7. Robot Mounting Stand

To evaluate candidate controllers, reliable physical safety assurance is necessary. Therefore, a Lexan safety shield was fabricated and attached to the robot stand. A safety factor of at least 3 of the safety shield's impact resistance was verified by dropping a 50-lb weight onto a sample of the test shield. Impacts were delivered with 3 times the robot's maximum kinetic energy with no observable damage to the shield.

Computer-Human Interface

To restore upper extremity function to individuals with high tetraplegia resulting from a spinal cord injury at or above the fourth cervical level (C3-C4), voluntary control signals must be obtained from the head or neck. Previous studies showed that EMG signals from the muscles of the head and neck and EOG signals from eyes are good candidates for control inputs.

Experiments were set up to record, process and evaluate EMG and EOG signals. Self-adhesive surface electrodes (from Kendall-LTP) were used to record EMG/EOG signals. The signals were amplified and filtered by CED-1902 amplifier modules (from CED Ltd) and digitized by a high-speed MultiQ-3 ADC card installed with the robot-control computer. Real-time signal-processing software adjusted the amplitude and bias of input signals to extract the voluntary control intents/commands from the subject.

Electrodes were placed above the subject's eyebrow to record the frontalis EMG signal. Experimental results show that the muscle contraction generates high EMG potential, and it takes around 0.5 second for the signal to drop back to a lower level. It is difficult for subjects to hold such EMG signals at a specific level, and the EMG signal tends to drift after successive muscle contractions. At a minimum, though, such signals should be effective for binary (on/off) input commands.

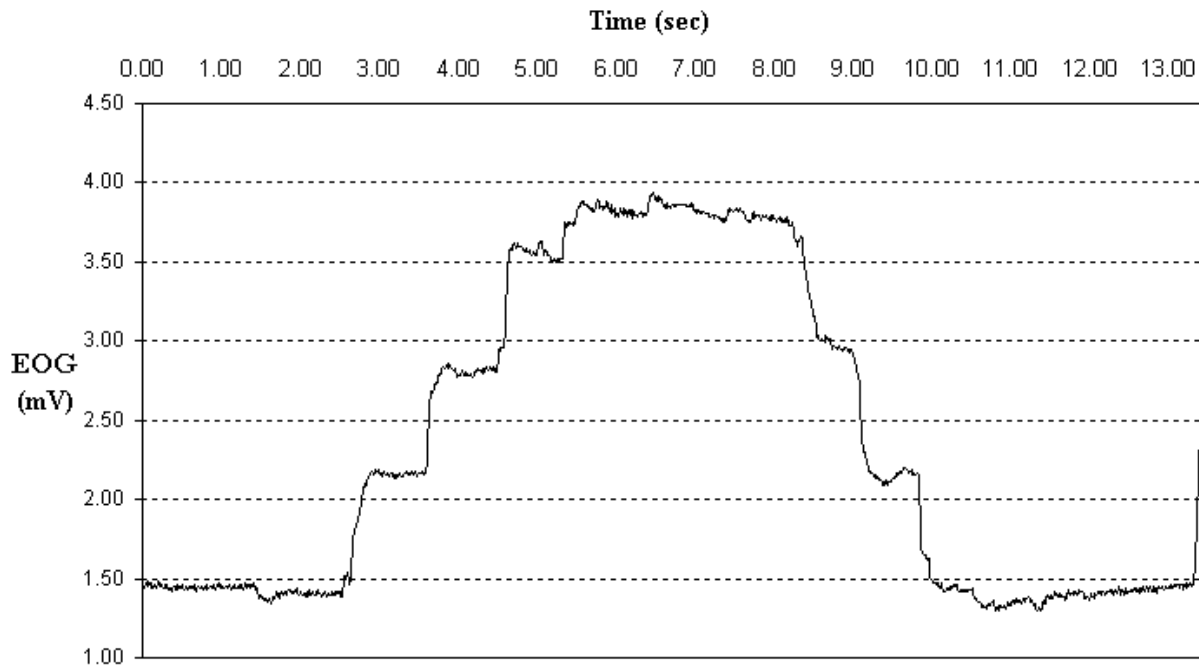


Figure 8. Horizontal EOG signal

Horizontal EOG's were recorded by placing two electrodes on the outside of the eyes, while a pair of electrodes were placed above and below an eye to detect vertical EOG signals.

Experiments show that EOG signals are linearly proportional to eye displacement. Further, eye velocities and accelerations can be determined from these signals. As shown in Figure 8, the horizontal EOG signal changed as the subject moved his eyes from left to the right and from right to the left. At the same time, holding a signal level is fairly easy for the subjects: the EOG signal holds its level when a subject fixes his eyes on an object. These properties are very attractive for use in future control schemes.

EOG signals can also be used to generate very sharp binary waveforms. Figure 9 shows that the subject generated EOG signals that could be interpreted as left clicks, right clicks, double-clicks and click-and-holds. These waveforms can be easily interpreted by computer software as a subject's voluntary motor commands.

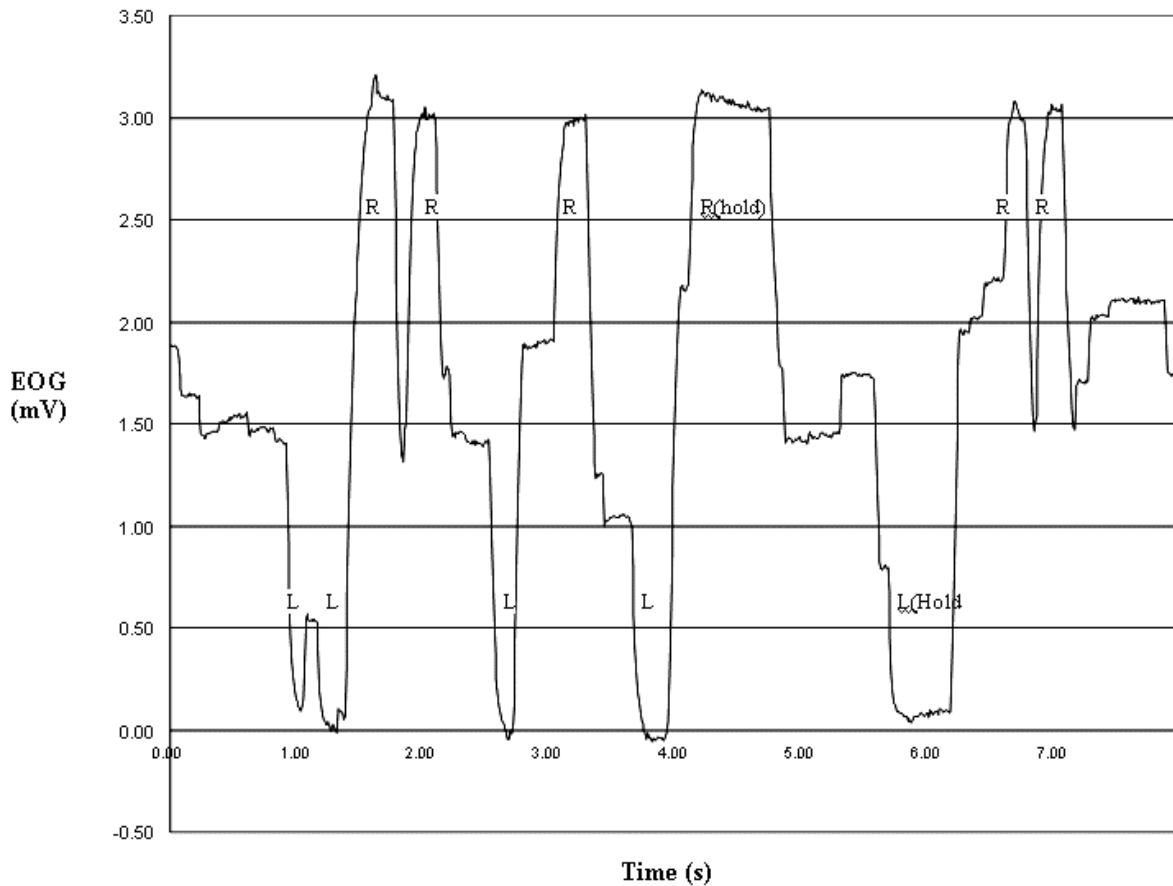


Figure 9. EOG signal for mode switching

A Robot Controller using EOG/EMG

A robot controller using EOG/EMG signals as command input sources was designed and tested. A protocol was designed to instruct subjects how to control the robot using EOG/EMG signal. After amplification, filtering and digitization, EMG/EOG signals were processed and interpreted conforming to the protocol. Horizontal EOG signals were interpreted as commands controlling the robot arm to move left and right horizontally; vertical EOG signals were used to

control the robot arm to move up and down; frontalis EMG signals were used to control the in-out motions.

Under the current test algorithm, as shown in Figure 10, if the EOG signal falls into the forbidden band, the robot won't move. When the signal is large enough, the robot will move at a constant speed. Therefore subjects can control the robot's motion in Cartesian space.

Figure 11 shows the controller using EMG/EOG as command input source. Currently, the subjects are controlling the robot motion in Cartesian space. Cylindrical space and joint space will be tested and evaluated in the next step.

Figure 10. Command interpretation

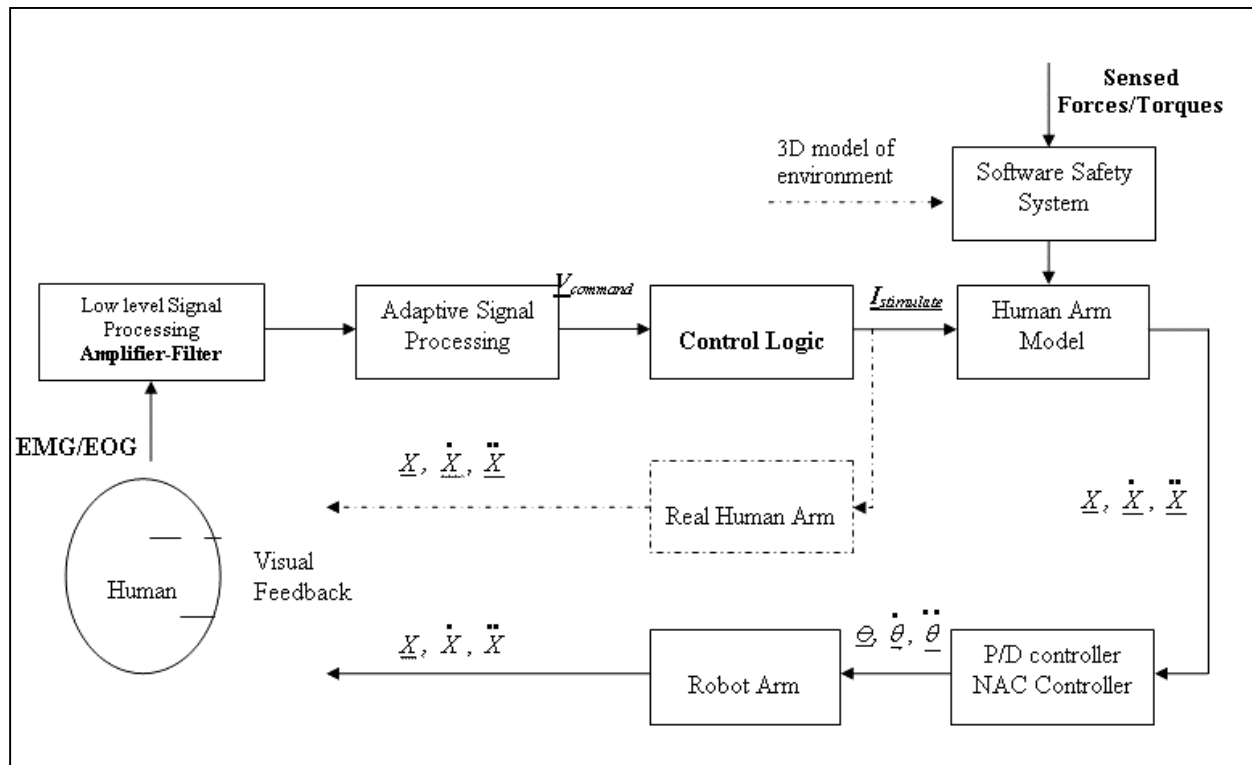
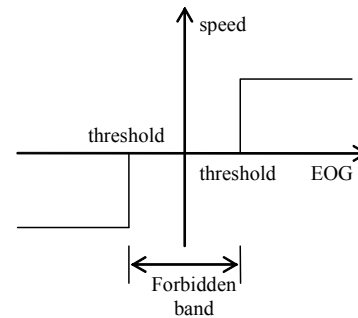


Figure 11. Robot controller using EMG/EOG

Next Quarter

To achieve better maneuverability, more control schemes will be designed and benchmarked during the next quarter. A series of tasks, such as controlling the robot to grab food, sort objects, etc., as well as the scoring standards will be defined. Subjects will be asked to try different tasks using a variety of control schemes. Environment force feedback will be included in the controller and compliant control will be explored, which is necessary when the robot interacts with the environment. In addition, the controller will incorporate a dynamic model of the human arm (under development) to produce more human-like (and more representative) arm motions.

Wireless data acquisition module for use with a neuroprosthesis

Contract section: E.1.a.v Sensory feedback of contact and grasp force

Abstract

The originally proposed plan of developing a thumbnail-mounted contact sensor that is connected to a small wireless transmitter has been altered so that now a general wireless data acquisition module is being developed. In addition to the thumbnail-mounted contact sensor, this general module could be utilized for other sensors used with a neuroprosthesis, such as the shoulder or wrist position transducer, finger-mounted joysticks, or remote on-off switches. Currently these sensors are connected to a controller via cables, which are cosmetically unappealing to the user and often get caught on wheelchairs, causing them to be damaged. Switch-activated transmitters mounted on walkers have been used previously in FES applications [1]. Recent advances in wireless technology have reduced the complexity and size of the wireless circuitry and have increased the likelihood that a small, low power, reliable wireless link could be assembled from commercially available components.

Methods

A set of desired specifications was developed for the wireless data acquisition module, including size, power consumption, transmission range, data rate, resolution and bandwidth requirements. A block diagram of the proposed wireless data acquisition module is shown in Figure 12. Available commercial wireless data acquisition devices were researched to see how well they fit the specifications of our application. In addition, commercial transmitter and transceiver development kits were investigated to determine the feasibility of developing a customized wireless module.

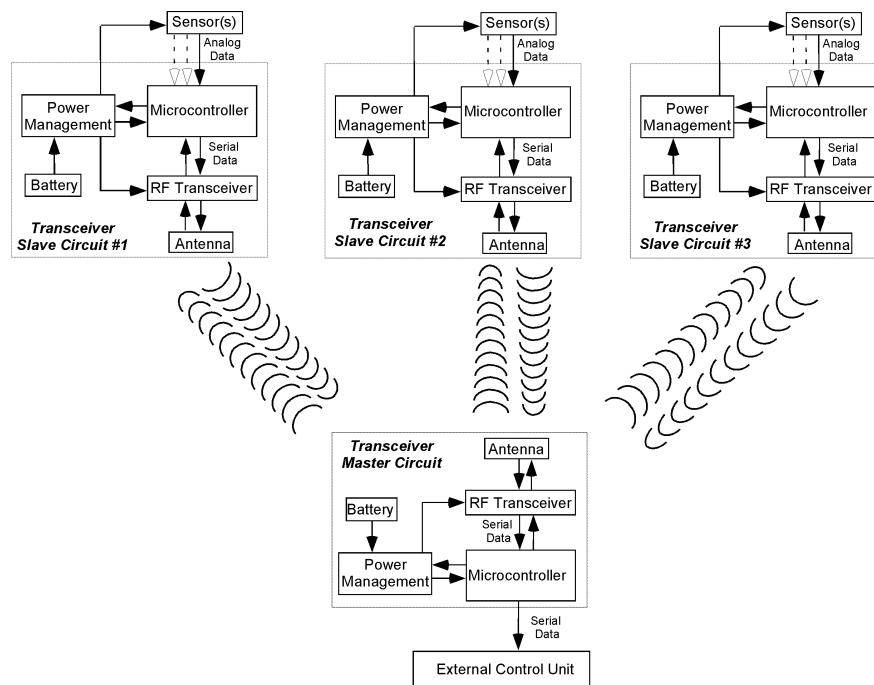


Figure 12. Wireless Data Acquisition Module Block Diagram

Results

After reviewing the available options, a three-pronged approach is being pursued.

1) Commercial wireless data acquisition devices:

Three commercial wireless data acquisition devices were identified as having specifications that were similar to our application: the StrainLink from MicroStrain Inc.; the RatPaak from Cleveland Medical Devices; and the i-Bean from Millennial Net. Although none of the devices satisfy all of our specifications, we have initiated discussions with the three companies about the possibility of customizing their devices.

2) Commercial transceiver development kit:

In case the above devices are not able to meet our needs, a small, low power transceiver module (the DR3000 from RF Monolithics) has been identified as an option for a customized wireless data acquisition module. A low-cost development kit is available that includes a microcontroller and communications software that should greatly reduce the development time for a customized device. The development kit and transceiver modules have been ordered.

3) Bluetooth wireless technology development kit:

Bluetooth wireless technology is a hardware and software specification that is being developed for low-power, short-range, personal area network communications. Its specifications, such as small size, low power, and high data rate are very attractive for our application. Hardware development kits are available. However, currently the software tools are limited and expensive. The availability of the software tools and development packages will be monitored to determine whether this can become a viable option for our application.

Next quarter

In the next quarter, the RF Monolithics development kit and transceiver modules should be received, and the appropriate software and hardware modifications will be started. In addition, communications with the three wireless data acquisition device vendors will continue to determine whether one of the commercially available devices can be customized to meet our specifications.

References

- [1] Z. Matijacic, M. Munih, T. Bajd, A. Kralj, H. Benko, and P. Obreza, "Wireless control of functional electrical stimulation systems," *Artif Organs*, vol. 21, pp. 197-200, 1997.

Rapid prototyping and real-time control for functional electrical stimulation (FES)

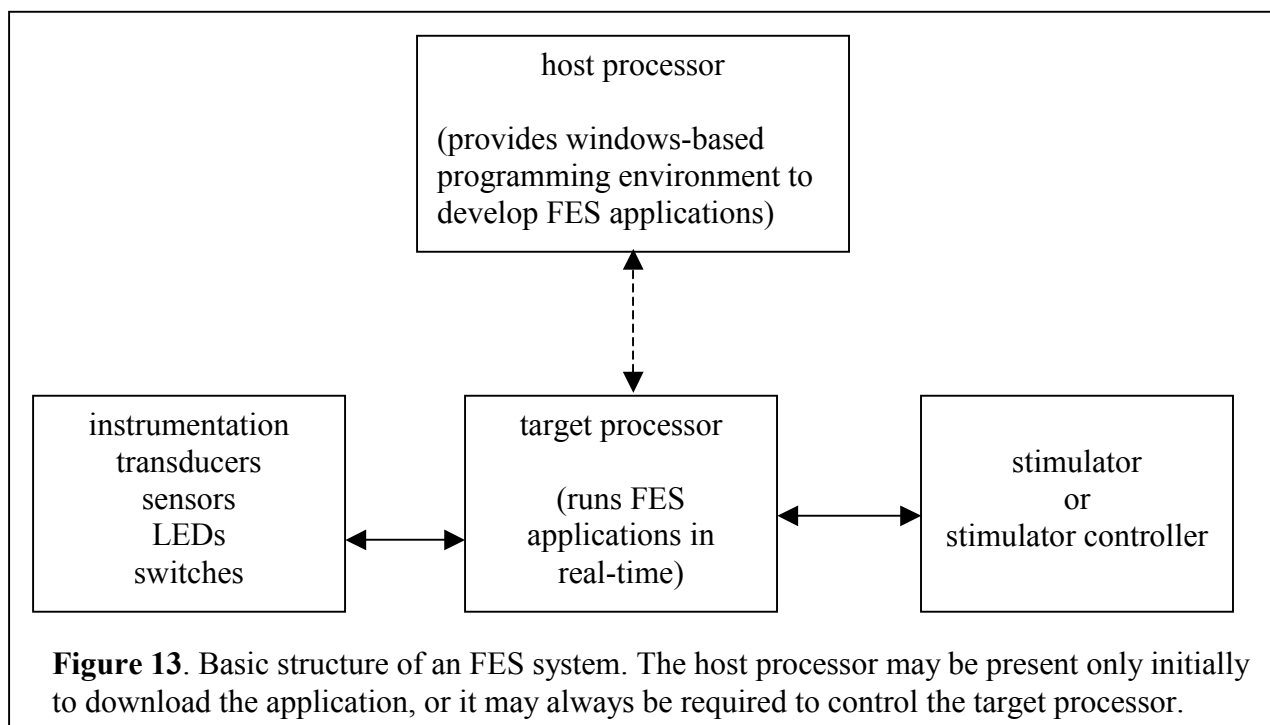
Contract section: E.1.a.vi Implementation and Evaluation of Neuroprosthesis for High Tetraplegia

Abstract

In this project, we are developing a set of software and hardware tools to provide rapid prototyping and real-time control for FES systems. The abilities to read physiological data, process and make calculations based on those inputs, then adjust and communicate stimulation parameters at repeatable, well-defined time intervals are essential to control and develop algorithms for neuroprostheses. Typically, only computer engineers or programmers using C and/or assembly language have achieved such real-time control. This moves the development effort away from the researchers and/or clinicians that are directly studying the system. By using the much higher level and more abstract means of programming required for software packages from The MathWorks [1-8], we aim to put into the hands of these users, themselves, the abilities to quickly design, implement, test, revise and re-test ideas in real-time. Our tools will provide a general mechanism for studying FES-related problems, and development of application-specific solutions using these tools will be left to individual researchers or clinicians. Therefore, we will be able to centralize the technology development and support for the core software and hardware that serve many projects in this contract. This reporting period represents the continued efforts at developing these tools. Described below are our basic setup and our first deliverable product.

Methods

A typical FES system is shown in Figure 13. The "Host Processor" provides a windows-based programming environment to develop FES applications. The "Target Processor" runs the FES applications in real-time. It also provides the interface(s) for various inputs and outputs. In order to provide rapid prototyping and real-time control, we use personal computers (PCs) running MathWorks software for the "Host" and "Target processors," as described in the last reporting period.



Interaction with laboratory equipment using factory-delivered and custom-built software

As described in the last reporting period, we developed a “one ch stim” (one channel stimulation) block and incorporated it into the Simulink Block Library. The “one ch stim” Graphical User Interface (GUI) has been improved to reflect the stimulus channel number, pulse period, and channel time offset for each occurrence of the block. The block also includes the ability to select the implant stimulator type as part of its initialization/setup. It will support both the IRS 8 and IST family of implant stimulators, but is presently hard-coded to work with the IRS 8 due to limited availability of IST emulators.

External Control Unit Development

The universal external control unit (UECU) is a portable system responsible for powering and acquiring data from various sensors and transducers, providing signal processing, implementing user control algorithms, and generating stimulus output through surface, percutaneous, and implanted systems. The UECU is based on a modular distributed processing architecture. This modularity allows the ECU to be configured as an application specific system consisting of only modules needed for a particular application. This realization also allows modifications to discrete sections of the entire system to be made without affecting the entire design and operation.

The UECU modules also provide the basis for the laboratory FES systems. The UECU Implant Control Module (ICM) is used to control the IRS 8 and IST family of implant systems. The ICM is used as the “stimulator controller” in the block diagram illustrated in Figure 13. The ICM can control two implant stimulators. During this reporting period a prototype ICM has been packaged for use in the laboratory and is shown in Figure 14 with an IRS 8 monitor box. The

UECU final form factor ICM has also been developed and is undergoing testing. It is shown in Figure 15 with the UECU Communications Module (CM).

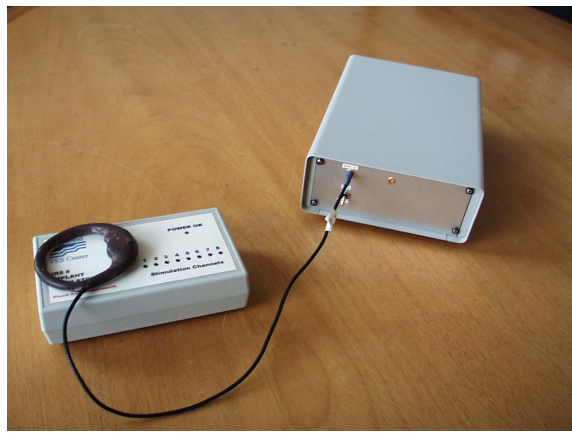


Figure 14. Laboratory based UECU Implant Control Module.

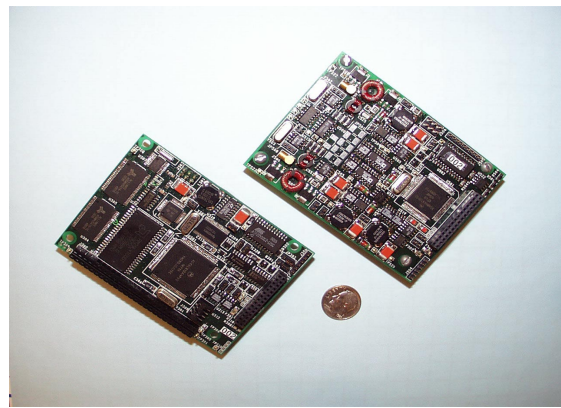


Figure 15. UECU Implant Communications Module (left) and Implant Control Module (right).

Results

Using the MathWorks tools, the enhanced "one ch stim" block, and the laboratory ICM, a multichannel stimulation algorithm was implemented to control multiple channels of an IRS 8 implant system in real-time. Multiple copies of the "one ch stim" block were used in the Simulink diagram to control the eight channels of an IRS 8 implant stimulator. The stimulus period and pulse offset were specified in the initialization/setup phase. The pulse duration and pulse current amplitude were specified as constants, but could be varied at any time. This control algorithm provided static outputs on all eight channels of the IRS 8. Various stimulus periods and channel offsets were tested.

A second control algorithm was implemented to read pulse duration data from a "Target Processor" A/D channel and proportionally control the pulse duration of one of the stimulus channels of the IRS 8. The Simulink block diagram is illustrated in Figure 16.

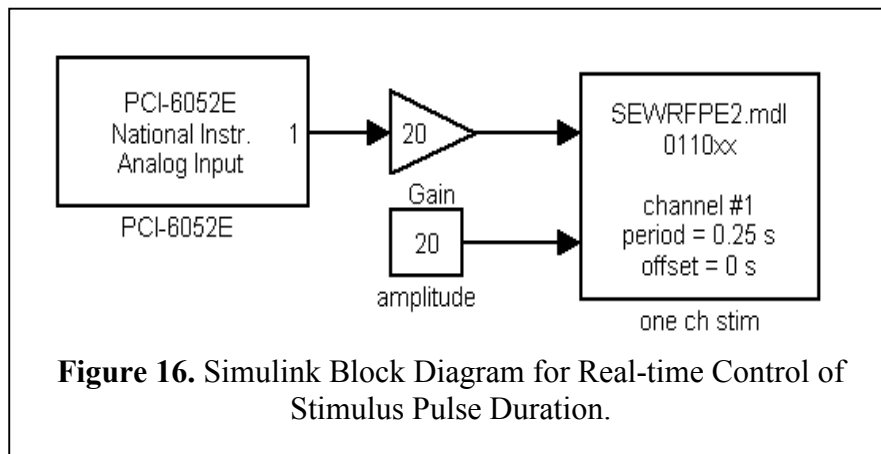


Figure 16. Simulink Block Diagram for Real-time Control of Stimulus Pulse Duration.

Next Quarter

The rapid prototyping software and hardware tools have been distributed to the various laboratories working under this contract. We will continue testing of the small form factor ICM and it will be integrated with the CM for enhanced performance.

References

1. Simulink, version 4.0, software release 12, The MathWorks Incorporated, Natick MA, June 2000.
2. Using Simulink (Version 4), The MathWorks Incorporated, Natick MA, 2000.
3. Real-Time Workshop, version 4.0, software release 12, The MathWorks Incorporated, Natick MA, March 2000.
4. Real-Time Workshop User's Guide (Version 4), The MathWorks Incorporated, Natick MA, 2000.
5. xPC Target, version 1.1, software release 12, The MathWorks Incorporated, Natick MA, June 2000.
6. xPC Target Getting Started Guide (Version 1), The MathWorks Incorporated, Natick MA, 2000.
7. MATLAB, version 6.0.0.88, software release 12, The MathWorks Incorporated, Natick MA, October 2000.
8. Using MATLAB (Version 6), The MathWorks Incorporated, Natick MA, 2000.